Single Molecule Detection by SERS of a Spaser-Based Bowtie Nanoantenna

Zhang Haopeng[1] Jiang Tao[1] Gao Yongfeng[2] Zhou Jun[1]

[1] *Department of Microelectronic Science and Engineering, Faculty of Science, Ningbo University, Ningbo, Zhejiang* 315211, *China*

[2] *Department of Optical Information Science and Technology, School of Mechanical Engineering, Jiangsu University, Zhenjiang, Jiangsu* 212013, *China*

Abstract Based on the mechanism of the surface plasmon amplification by stimulated emissions of radiation (spaser), a bowtie nanoantenna structure is proposed for single molecule detection by surface enhanced Raman scattering (SERS). The localized surface plasmon resonance (LSPR) properties and the SERS characteristics of the bowtie nanoantenna are numerically analyzed by the finite element method (FEM). The results show that the LSPR strength and the local electric field intensity of the bowtie nanoantenna can be greatly amplified, and its scattering cross-section and electric field strength are up to 1.1×10^4 and 1×10^2 times of the non-spaser bowtie nanoantenna, respectively. Meantime, the maximum SERS enhancement factor is 10^{16} generated by the bowtie nanoantenna, which is enough to accurately detect a single molecule. Moreover, there is a higher SERS enhancement factor of 10^{12} on the entire surface of the nanoantenna, which is also sufficient for single bio-molecular detection.

Key words spectroscopy; surface enhanced Raman scattering; single molecule detection; surface plasmons; nanomaterials

OCIS codes 240.6695; 120.1880; 240.6680; 160.4236

表面等离子体受激辐射放大领结型纳米天线的 SERS 单分子探测

张昊鹏[1] 姜 涛[1] 高永峰[2] 周 骏[1]

[1]宁波大学理学院微电子科学与工程系，浙江 宁波 315211

[2]江苏大学机械工程学院光信息科学与技术系，江苏 镇江 212013

摘要 基于表面等离激子受激辐射放大原理，提出了一种应用于表面增强拉曼散射(SERS)单分子探测的领结型纳米天线结构。采用有限元方法(FEM)研究其局域表面等离子体共振(LSPR)和 SERS 特性。结果表明，该领结型纳米天线的局域表面等离子体共振强度和局域电场强度得到明显的增强，其散射截面为非表面等离激子受激辐射放大领结型纳米天线的 1.1×10^4 倍，局域电场强度为 1×10^2 倍。同时，该领结型纳米天线的表面增强拉曼散射增强因子最大达到 10^{16}，足以进行精确的单分子探测；整个纳米天线表面的增强因子也可达到 10^{12}，足以应用于单个生物分子的探测。

关键词 光谱学；表面增强拉曼散射；单分子探测；表面等离子体；纳米材料

中图分类号 O433.4 **文献标识码** A **doi**：10.3788/CJL201441.0908002

收稿日期：2014-01-13；**收到修改稿日期**：2014-03-03

基金项目：国家自然科学基金(61275153)、浙江省自然科学基金(LY12A04002)、浙江省“物理学重中之重学科”开放基金(xkzl1208)、宁波市自然科学基金(2012A610107)、宁波大学优秀学位论文培育基金(PY2012006)

作者简介：张昊鹏(1990－)，男，硕士研究生，主要从事金属介质纳米粒子局域表面等离子体方面的研究。E-mail：zhp364117036@sina.com

导师简介：周 骏(1958－)，男，教授，博士生导师，主要从事光学与光电子学方面的研究。E-mail：zhoujun@nbu.edu.cn(通信联系人)

本文电子版彩色效果请详见中国光学期刊网 www.opticsjournal.net

1 Introduction

Surface enhance Raman scattering (SERS) has attracted great scientific and technological interest as an effective detection tool of single molecule due to its high sensitivity and molecular specificity[1-3]. As we have known, the mechanism of SERS can be described as: the local surface plasmon resonance (LSPR) induced by the strong oscillation of conduction electrons on the surface of noble metal nanostructures leads to a strong enhancement of the local electric field intensity when the nanostructure is excited by an incident light, which makes the Raman signals of molecules attached on the nanostructure to be enhanced extremely[4-5]. Recently, more great attentions have been focused on SERS characteristics of complex nanosystem such as the nanoparticle aggregates to realize single molecule detection[6-12], because a great amount of "hot spots" in the nanoparticle aggregates can generate the enhancement factor of SERS signal (G factor) to $10^{11}\sim10^{15}$[6-9]. However, considering the technical cost, most of nanoparticle aggregates have been synthesized by chemical method, which means they are hard to be prepared precisely and repeatably. Fortunately, there is another way to obtain a high G factor, that is, the small edge of metal nanostructure can induce a huge local electric field intensity, which is known as "tip effect"[10]. And, the "tip effect" is highly dependent on the different configurations, sizes and morphologies of noble metal nanostructures[11-12]. Especially, a bowtie nanoantenna system can generate "hot spot" and "tip effect" in the gap between the two gold triangle tips, simultaneously[13]. Meanwhile, by using the electron beam lithography (EBL)[14] and the light lithography methods[15-16], the experimental fabrication of bowtie nanoantenna is convenient, precise and repeatable. Therefore, various bowtie nanoantenna systems are of great interests in realizing single molecule detection by SERS.

On the other hand, it is worth noting that the mechanism of surface plasmon (SP) amplification by stimulated emission of radiation (spaser), proposed by Bergman *et al*. in 2003[17], can be applied in sensing field, as our viewpoint. In fact, it is the gain material coated on the surface of nanoparticles providing the energy to completely compensate the propagation loss of SP in spaser structure by means of energy transfer from gain material to metal, which finally forms the SP amplification. Many researchers have demonstrated theoretically and experimentally that the SP amplification is very sensitive to the gain threshold, and the local electric field intensity can be highly improved[17-19]. Therefore, constructing a spaser-based metal nanostructure with an enough high G factor is feasible to realize single molecule detection.

In this letter, we propose a spaser-based bowtie nanoantenna with gold shell and gain material doped core, and then demonstrate its great enhancement of scattering strength and local electric field intensity. By carefully numerical simulating and optimal designing, it is found that the spaser-based bowtie nanoantenna possesses a G factor of $10^{12}\sim10^{16}$, which generates SERS sufficiently for single molecule detection. All calculations are performed using a computational electrodynamics modeling technique based on the finite element method (FEM), due to the good precision in resolving nanoscale electromagnetic fields near metal-dielectric nanostructure[19-20].

2 Model and theroy

The configuration of the spaser-based bowtie nanoantenna is shown in Fig. 1, which is composed by a pair of equilateral triangular gold nanoshells and silica core doped with a gain material. In consideration of the feasibility of practical fabrication[13-16] and the efficiency in single molecule detection[5], the length, the height and the thickness of the equilateral triangular gold shell are set as L = 100 nm, H = 40 nm and T = 5 nm, respectively. The gap distance between the two equilateral triangular components is D = 10 nm. For simplicity, the refractive index of the silica in the gold shells is set as $n_{\text{silica}} = 1.5 - \mathrm{i}k$, where k is the optical loss/gain coefficient for describing the dissipation/amplification of the incident light intensity in the silica media[18, 21]. The dielectric constant of gold is obtained from the experimental data of Johnson and Christy[22]. The medium surrounding of the bowtie nanoantenna is air with the refractive index n_0 = 1.0. Congruently, the incident light propagating along the x-axis is polarized parallel to the z-axis.

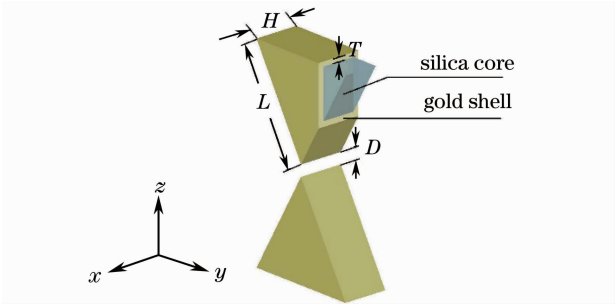

Fig. 1 Schematic of the spaser-based bowtie nanoantenna (the angle uncovered gold is drawn to expose silica core in the gold shell)

The scattering and absorption properties of the bowtie nanoantenna are numerically studied in the frequency domain using the scattering field formulation. Due to the precision and the efficiency of the FEM method in solving electric field distribution of nanostructures, all the simulations are obtained by using a commercial FEM package (COMSOL mutiphysics 4.3 with the radio frequency module). The scattering cross-section C_{scat} is integrated by the normalized electric field around a far-field transform boundary enclosing the whole system[23]:

$$C_{\mathrm{scat}}=\frac{1}{E_{\mathrm{inc}}^{2}}\int|E_{\mathrm{far}}|^{2}\mathrm{d}S, \tag{1}$$

where $\boldsymbol{E}_{\mathrm{far}}$ is the far-field electric component of the scattering field calculated by the COMSOL implementation of the Stratton-Chu formula[20] and $\boldsymbol{E}_{\mathrm{inc}}$ is the incident electric field amplitude. Absorption cross-section is obtained by intergrating the time-average resistive heating (U_{av})[24]:

$$C_{\mathrm{abs}}=\frac{2}{\sqrt{\varepsilon_0/\mu_0}E_{\mathrm{inc}}^{2}}\int U_{\mathrm{av}}\mathrm{d}V, \tag{2}$$

where ε_0 and μ_0 are permittivity and permeability of vacuum respectively. $U_{\mathrm{av}}=\frac{1}{2}\mathrm{Re}(\sigma\boldsymbol{E}\cdot\boldsymbol{E}^{*}-\mathrm{j}\omega\boldsymbol{E}\cdot\boldsymbol{D}^{*})$, σ is the conductivity of the integrated material, ω, E and D are angular frequency, electric field verctor and electric displacement vector of the incident light, repectively.

3 Results and discussions

3.1 Optical properties of the bowtie nanoantenna

From Eqs. (1)～(2), the scattering and absorption spectra of the bowtie nanoantenna are calculated by the optical cross-sections C_{scat} and C_{abs} at different values of k and shown in Fig. 2. When $k=0$ [Fig. 2 (a)], corresponding to undoped gain material, both scattering and absorption peaks of the bowtie nanoantenna locate at 888 nm, and the linewidth of the peaks is 60 nm. Meanwhile, the maximum value of C_{abs} is much larger than that of C_{scat}, which means the energy from the incident light is consumed due to the surface plasmon loss of gold nanoshelles without availably compensated. In addition, because of the strong dissipation of conduction electrons on the surfaces of gold nanoshelles, the quality factor (Q) of the bowtie nanoantenna is low (about 10), which indicates that the spaser-based bowtie nanoantenna maintains a low ratio of energy stored to offset the dissipated loss. However, when k takes effect by doping silica with gain material, the optical cross-section spectra are quite different from those when $k=0$, as identified in Fig. 2(b)～(f). When $k=0.25$, C_{scat} increases distinctively but C_{abs} decreases due to the energy loss of the gold shell partial compensated by the gain material in silica core, and the linewidths reduce to only about 30 nm. When $k=0.45$, scattering is greatly enhanced and the peak value of C_{scat} is about 67 times as large as the value when $k=0$. C_{abs} shows

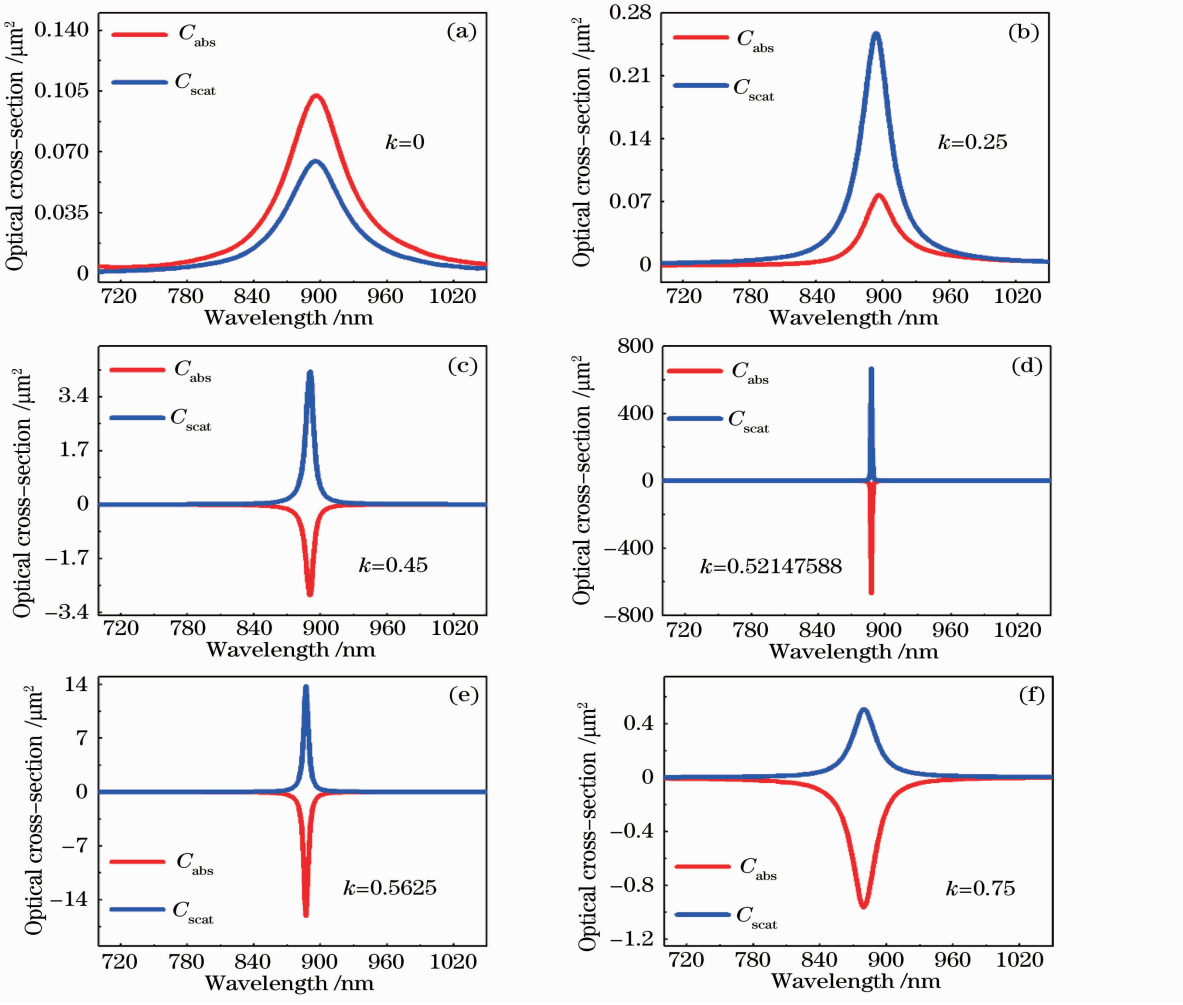

Fig. 2 Optical cross-section spectra of the spaser-based bowtie nanoantenna with different k

negative value due to compensating the energy loss of surface plasma in the gold shell by energy resonance transmission from the gain material to the gold shell, and the line widths decrease to about 8 nm. It is worth noting that, when k further increases to a critical value, $k=0.52147588$, a super-resonance emerges[18, 21]. The peak value of C_{scat} jumps to a maximum of 667.15 μm^2 and the peak value of C_{abs} drops to a minimum of -667.15 μm^2, which are 1.1×10^4 times and -7×10^3 times as much as the undoped bowtie nanoantenna, respectively. Meanwhile, the linewidths abruptly decrease to less than 1 nm. At the same time, there is four orders of magnitude enhancement of LSPR properties of gold nanoshell and the energy loss is completely compensated by light amplification from the gain material. Consequently, the quality factor is greatly improved and the net amplification of the spaser-based bowtie nanoantenna is zero as a result of the balance between loss and gain, so that a stable operating spaser mechanism can be effectively established[17]. When k continues to increase until slightly beyond the critical value as shown in Fig. 2(e), $k=0.526$, the LSPR of the spaser-based bowtie nanoantenna falls rapidly away from the super-resonance, and the peak values of C_{scat} and C_{abs} abruptly change to 13.71 μm^2 and -16.075 μm^2, and their peak linewidths increase to 4 nm. If k further increases to 0.75, absorption dominates over scattering from the gold nanoshells and the linewidths of absorption peak extend to 22 nm, leading to a net amplification of light and a sharp decline in the quality factor due to the absence of resonance energy transfer in the bowtie nanoantenna.

To show the dependence of LSPR strength on the gain coefficient, C_{scat} and C_{abs} spectra are plotted as functions of k at the resonance wavelength of 888 nm (Fig. 3). It is clear that, the super-resonance emerges at the critical point of k. Departing slightly the super-resonance peak at $k=0.52147588$, C_{scat} and C_{abs} are abruptly magnified and then fell to nearly zero, which is similar to the case of $k=0$. Therefore, it is reasonable

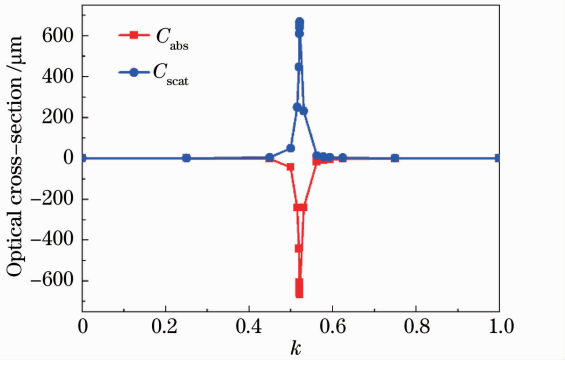

Fig. 3 Scattering cross-section and absorption cross-section of the spaser-based bowtie nanoantenna as a function of k at LSPR wavelength

to regard $k=0.52147588$ as athreshold, k_{thre}, which can be used for establishing effective LSPR amplification.

The above results can be easily understood from the spaser mechanism which describes the surface plasmon amplificationas result of interactions among the doped gain material in silica, gold nanoshell, and the incident light[5,17-18,21]. The above dynamic interaction processes are described as follow: the gain material provides energy to compensate the surface plasmon loss in the gold nanoshell or forms the surface plasmon amplified output, and in return, the LSPR mode regulates photons in the doped silica by means of strength-related feedback[21]. When k is below the threshold, the gain material does not change the physical property of the LSPR mode of the gold nanoshell but absorbs energy from the incident light, and the quality factor remains low. However, when k reaches the threshold, the energy absorbed by the gain material can completely transfer to the LSPR mode by energy resonance, and then magnifies the SP energies by LSPR-mode coupling[18]. A relative balance between the energy loss of gold nanoshell and the amplification of gain material is arrived, naturally, a super-resonance will emerge and the net amplification is zero. At this point, the spaser-based bowtie nanoantenna has a high quality factor and the resonance linewidths rapidly diminishes due to the efficient photo-plasmon coupling. It is similar to the LSPR in a dynamic high-quality nanocavity where the accumulation effect can greatly increase the LSPR[5]. If k further increases, the energy loss and the gain compensation in the bowtie nanoantenna will be broken, and the stable spaser mechanism will not emerge as well as the amplification of LSPR[5,18].

3.2 Single molecule detection by SERS

For Fig. 4(a), $k=k_{thre}$, the electric field intensity near the tips of the gold nanoshell, called "hot spot" area of the bowtie nanoantenna, is greater than thoes of other regions. The maximum value of electric field at the "hot spot" area is 1.2167×10^4, while the electric field values at the gold triangle nanoshell edges are only about 1.5×10^3. The electric field distribution indicates that the electric field of the gap between the two gold nanoshells is greatly enhanced. To clearly describe the electric field distribution of the "hot spot" area, a partial enlarged view of the electric field pattern of the gap between the two gold nanoshells is shown in Fig. 4 (b). It displays an obvious difference of the electric field intensity between the "hot spot" area and the other areas. In addition, the electric field strength of the "hot spot" decreases gradually from its center to its edge. To illustrate the great enhancement of the electric field intensity, the electric field distribution of the spaser-based bowtie nanoantenna at $k=0$ is shown in Fig. 4 (c). The maximum value of the electric field intensity near the tips is only 115.02, and there is no "hot spot" in the gap between the two gold nanoshells. By

changing the display range of electric field intensity, as shown in Fig. 4(d), the entire surface of the bowtie nanoantenna covered by a complete electric field distribution pattern exhibited a higher electric field intensity. In fact, the great enhancement of the electric field intensity of the spaser-based bowtie nanoantenna can be attributed to the spaser mechanism, "hot spot" and "tip effect" of surface plasma in metal nanostructure. "Hot spot" at the junction between the adjacent nanoparticles denotes a high local electric field from the nearest-neighbor coupling between the LSPR modes which is excited by incident light with appropriate polarization[25-26]. And, such high-intensity regions is also owing to "tip effect", that is the high local-field enhancement at sharp corners or small curvatures of metal nanostructure, due to the amplification of their LSPR resulting from the accumulation of the conduction electrons under radiating light[10-11]. In addition, when the spaser mechanism is established in the metal nanostructure, the effective amplification of the LSPR mode by energy resonant transimission between the gain material and the metal can further reinforce the intensity of the electric field in the juction between adjacent metal nanosystems or the tip regions. Therefore, the spaser-based bowtie nanoantenna combines the "hot spot", the "tip effect" and the spaser mechanism to drastically enhance the intensity of the electric field in the metal nanostructure, especially around the tips of the gold nanoshelles, which is crucial to realize a great G factor for single molecule detection by SERS.

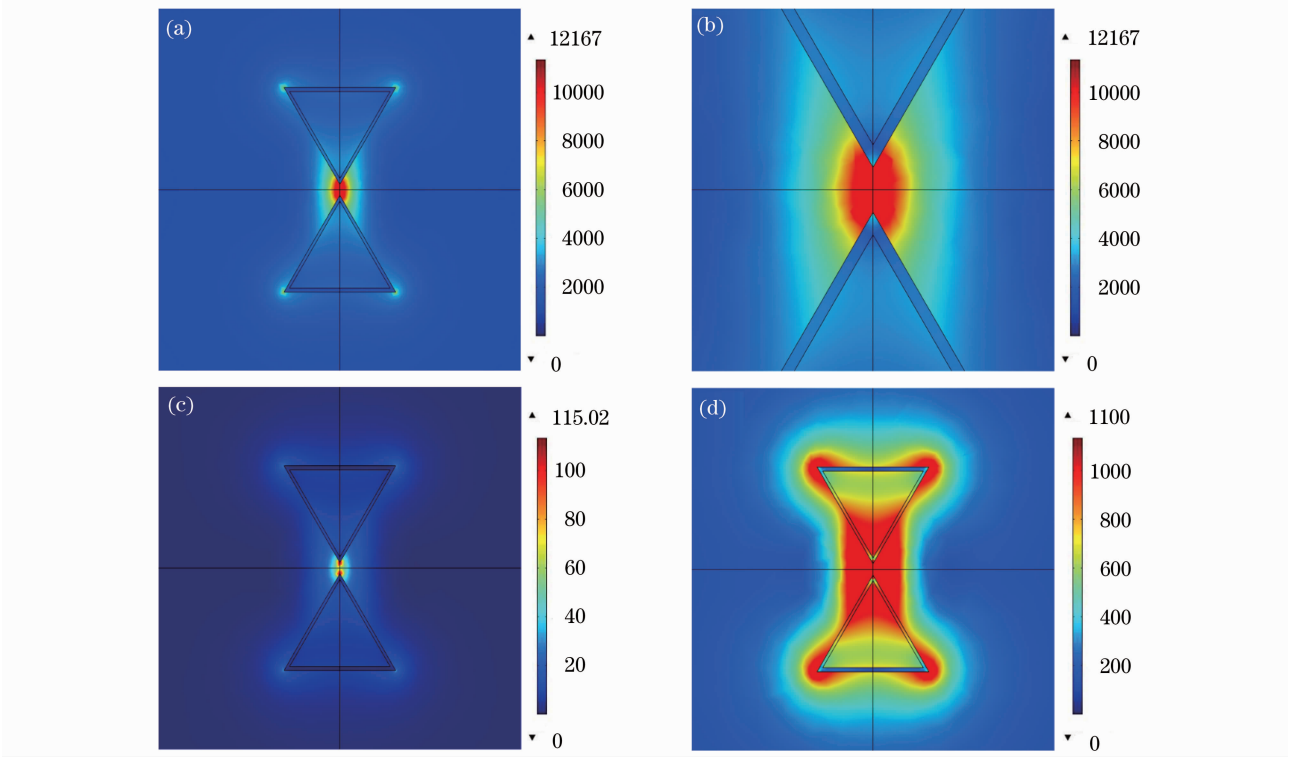

Fig. 4 Electric field distributions of the spaser-based bowtie nanoantenna in y-z plane. (a) $k = 0.52147588$; (b) enlarged "hot spot" area between two tips of the gold nanoshelles; (c) $k = 0$; (d) intensity display of the case of $k = 0.52147588$ in the range of 0～1100 rule

The electromagnetic effect is the mainly factor of the spaser-based bowtie nanoantenna to realize single molecule detection by SERS. Here, the electromagnetic factor, G factor is introduced for quantifying the influences of the electromagnetic effect on the SERS signal[4-5]. G factor describes the enhancement of the optical field due to the excitation of LSPR in the metallic nanostructures and can be expressed as[5]

$$G(r_m, \nu) = |E(r_m, \nu)/E_{inc}(\nu)|^4, \quad (3)$$

where $E(r_m, \nu)$ is the total electric field at the coordinate r_m at the incident light frequency ν, $E_{inc}(\nu)$ is the incident excitation field. G factor as a function of gain coefficient k at the resonance wavelength is plotted in Fig. 5. At the point of the super resonance, $k = k_{thre}$, G factor reaches its maximum value, 2.1915×10^{16}, eight orders of magnitudes higher than the undoped one, which is sufficient for single molecule detection. Even the maximum value of the electric field intensity is 1100, as shown in Fig. 4(d), a maximum value 1.7502×10^{12} of G factor is four orders of magnitudes higher than that in Fig. 4(a). Although it is hard to locate the molecule in the maximum region of the electric field, G factor of the entire surface of the bowtie nanoantenna can even reach a sufficient high level for practical single molecule detection.

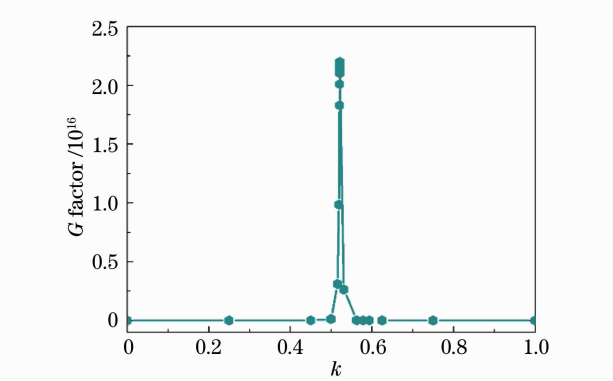

Fig. 5 G factor of the spaser-based bowtie nanoantenna versus gain coefficient k at the resonant wavelength of 888 nm

4 Conclusions

A spaser-based bowtie nanoantenna is theorectically proposed for single molecule detection by SERS. It is found that, the strength of LSPR of gold nanoshell is greatly enhanced by introducing the spaser mechanism. The scattering cross-section of the bowtie nanoantenna is 1.1×10^4 times and the local electric field intensity is higher up to two orders of magnitudes comparing with that of the non-spaser one. Meanwhile, the high local electric field intensity is around the bowtie nanoantenna, which is feasible for single molecule detection beyond the "hot spot". Furthermore, a maximum 2.1915×10^{16} of G factor is calculated for the spaser-based bowtie nanoantenna. By introducing the spaser mechanism, both the electric field intensity in "hot spot" and entire surface of the bowtie nanoantenna with doped gain material can be greatly enhanced to generate strong SERS signal for realizing single molecule detection. Therefore, the spaser-based bowtie nanoantenna has a very promising potenial for accurate, efficient and comprehensive single molecule detection by SERS.

References

1 M Martin. Surface-enhanced spectroscopy[J]. Rev Mod Phys, 1985, 57(3): 783 - 826.

2 A Campion, P Kambhampati. Surface-enhanced Raman scattering [J]. Chem Soc Rev, 1998, 27(7): 241 - 250.

3 C L Haynes, A D McFarland, R P Van Duyne. Surface-enhanced Raman spectroscopy[J]. Analytical Chemistry, 2005, 77(17): 339 - 346.

4 K Keipp, Y Wang, H Kneipp, *et al*.. Single molecule detection using surface-enhanced Raman scattering (SERS)[J]. Phys Rev Lett, 1997, 78(9): 1667 - 1670.

5 Z Li, Y Xia. Metal nanoparticles with gain toward single-molecule detection by surface-enhanced Raman scattering[J]. Nano Lett, 2010, 10(1): 243 - 249.

6 P Muhlschlegel, H J Eiler, O J F Martin, *et al*.. Resonant optical antennas[J]. Science, 2005, 308(10): 1607 - 1609.

7 A Sundaramurthy, K B Crozier, G S Kino. Field enhancement and gap-dependent resonance in a system of two opposing tip-to-tip Au nanotriangles[J]. Phys Rev B, 2005, 72(16): 165409.

8 J Britt Lassiter, Javier Aizpurua, Luis I Hernandez, *et al*.. Close encounters between two nanoshells[J]. Nano Lett, 2008, 8(4): 1212 - 1218.

9 H Xu, E J Bjerneld, M Käll, *et al*.. Spectroscopy of single hemoglobin molecules by surface enhanced Raman scattering[J]. Phys Rev Lett, 1999, 83(21): 4357 - 4360.

10 B Pettinger, B Ren, G Picardi, *et al*.. Nanoscale probing of adsorbed species by tip-enhanced Raman spectroscopy[J]. Phys Rev Lett, 2004, 92(9): 096101.

11 E G Bortchagovsk, S Lein, U C Fischer. Surface plasmon mediated tip enhanced Raman scattering[J]. Appl Phys Lett, 2009, 94(6): 063188.

12 E G Bortchagovsky, U C Fischer. A retrahedral tip as a probe for tip-enhanced Raman scattering and as a near-field Raman probe [J]. J Raman Spectroscopy, 2009, 40(10): 1386 - 1391.

13 N A Hatab, C Hsueh, A L Gaddis, *et al*.. Free-standing optical gold bowtie nanoantenna with variable gap size for enhanced Raman spectroscopy[J]. Nano Lett, 2010, 10(12): 4952$_4$955.

14 Feng Yaping, Zhou Jun, Yang Mingyang, *et al*. Fabrication and optical properties of two-dimensional thue-morse quasicrystals[J]. Acta Optica Sinica, 2011, 31(4): 0423001.
冯亚萍,周　骏,阳明仰, 等. 二维 Thue-Morse 型准周期光子晶体的制作与光学特性[J]. 光学学报, 2011, 31(4): 0423001.

15 Lu Dunwu, Huang Huijie, Yan Yu, *et al*.. Deep submicron excimer laser lithography[J]. Acta Optica Sinica, 1996, 16(8): 1169 - 1172.
路敦武,黄惠杰,鄢　雨, 等. 深亚微米激光光刻研究[J]. 光学学报, 1996, 16(8): 1169 - 1172.

16 Mei Longhua, Zhou Jinyun, Lei Liang, *et al*.. Measurement and evaluation for the optical system in laser large-area scanning projection imaging lithography [J]. Laser & Optoelectronics Progress, 2012, 49(7): 072201.
梅龙华,周金运,雷　亮, 等. 激光光刻大面积扫描投影成像光学系统测试及评价[J]. 激光与光电子学进展, 2012, 49(7): 072201.

17 D J Bergman, M I Stockman. Surface plasmon amplification by stimulated emission radiation: quantum generation of coherent surface plasmons in nanosysytems[J]. Phys Rev Lett, 2003, 90(2): 027402.

18 H Zhang, J Zhou, W Zou, *et al*.. Surface plasmon amplification characteristics of an active three-layer nanoshell-based spaser[J]. J Appl Phys, 2012, 112(7): 074309.

19 A L Koh, K Bao, I Khan, *et al*.. Single silver nanoparticles and dimers: influence of beam damage and mapping of dark modes[J]. ACS Nano, 2009, 3(10): 3015 - 3022.

20 Y Fang, Z Li, Y Huang, *et al*.. Branched silver nanowires as controllable plasmon routers[J]. Nano Lett, 2010, 10(5): 1950 - 1954.

21 S Liu, J Li, F Zhou, *et al*.. Efficient surface plasmon amplification from gain-assisted gold nanorods[J]. Opt Lett, 2011, 36(7): 1296 - 1298.

22 P B Johnson, R W Christy. Optical constants of the noble metals [J]. Phys Rev B, 1972, 6(12): 4370 - 4379.

23 M W Knight, N J Halas. Nanoshells to nanoeggs to nanocups: optical properties of reduced symmetry core-shell nanoparticles beyond the quasistatic limit[J]. New J Phys, 2008, 10(10): 105006.

24 J A Stratton. Electromagnetic Theory[M]. New York: McGraw-Hill, 1941.

25 C E Talley, J B Jackson, C Oubre, *et al*.. Surface-enhanced Raman scattering from individual Au nanoparticles and nanoparticles dimer substrates[J]. Nano Lett, 2005, 5(8): 1569 - 1574.

26 S Grésillon, L Aigouy, A C Boccara, *et al*.. Experimental observation of localized optical excitation in radom metal-dielectric films[J]. Phys Rev Lett, 1999, 82(22): 4520 - 4523.

栏目编辑: 史　敏